Supporting Information

Efficient hydrogen generation from formic acid using AgPd nanoparticles immobilized on carbon nitride-functionalized SBA-15

Lixin Xu[a], Bo Jin[a], Jian Zhang[a], Dang-guo Cheng[b], Fengqiu Chen[b], Yue An[b], Ping Cui[a] and Chao Wan [a,*]

[a] *College of Chemistry and Chemical Engineering, Anhui University of Technology, 59 Hudong Road, Ma'anshan 243002, China*

[b] *College of Chemical and Biological Engineering, Zhejiang University, 38 Zheda Road, Hangzhou 310027, China*

---

* Corresponding author. Tel.: +86 555 2311807; Fax: +86 555 2311822.

E-mail address: wanchao1219@hotmail.com (Chao Wan)

Calculation methods:

$$x_a = \frac{P_{atm}V_{H2}/RT}{n_{FA}} \quad \text{(S1)}$$

Where x_a is conversion, P_{atm} is the atmospheric pressure (101325 Pa), V_{H2} is the generated volume of H_2, R is the universal gas constant (8.3145 $m^3 \cdot Pa \cdot mol^{-1} \cdot K^{-1}$), T is room temperature (278 K), and n_{FA} is the mole number of FA.

$$TOF_{initial} = \frac{P_{atm}V_{H2}/RT}{n_{Ag+Pd}\,t} \quad \text{(S2)}$$

Where $TOF_{initial}$ is initial turnover frequency when x_a reaches 20%, n_{Ag+Pd} is the mole number of the Ag and Pd, and t is the reaction time when x_a reaches 20%.

(S1) Y. Yuan, Z. Zhao, J. Zheng, M. Yang, L. Qiu, Z. Li and Z. Zou, J. Mater. Chem., 2010, 20, 6772.

(S2) P. Chen, T. Y. Xiao, H. H. Li, J. J. Yang, Z. Wang, H. B. Yao and S. H. Yu, ACS Nano., 2012, 6, 712.

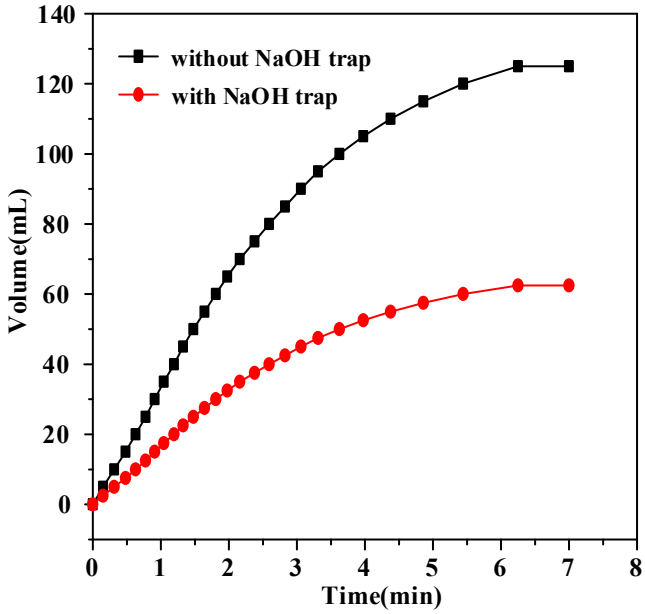

Fig. S1. Gas generation by decomposition of FA/SF vs time catalyzed by $Ag_{10}Pd_{90}$/0.2CND/SBA-15 at 323 K with and without NaOH trap (catalyst= 100 mg, n_{FA} =3 mmol, n_{SF} =1 mmol).

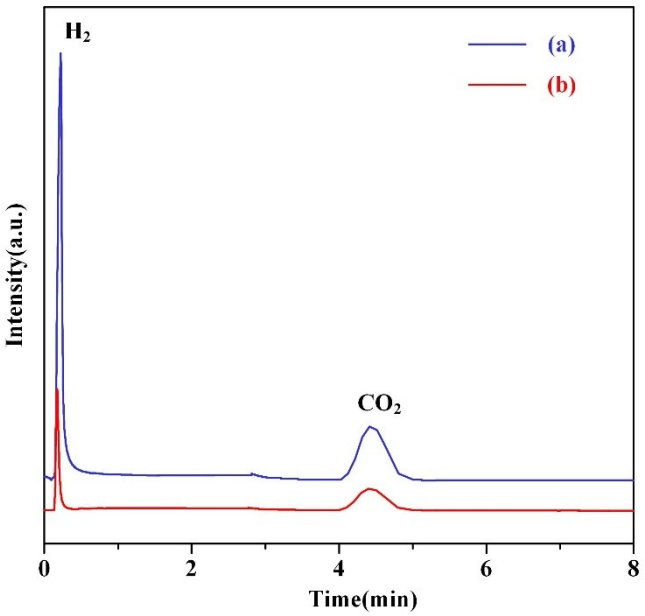

Fig. S2. GC spectrum using TCD for a) commercial mixture gas of H_2 and CO_2, and b) evolved gas from FA/FS aqueous solution (n_{FA} =3 mmol, n_{SF} = 1 mmol) over $Ag_{10}Pd_{90}$/0.2CND/SBA-15 at 323 K.

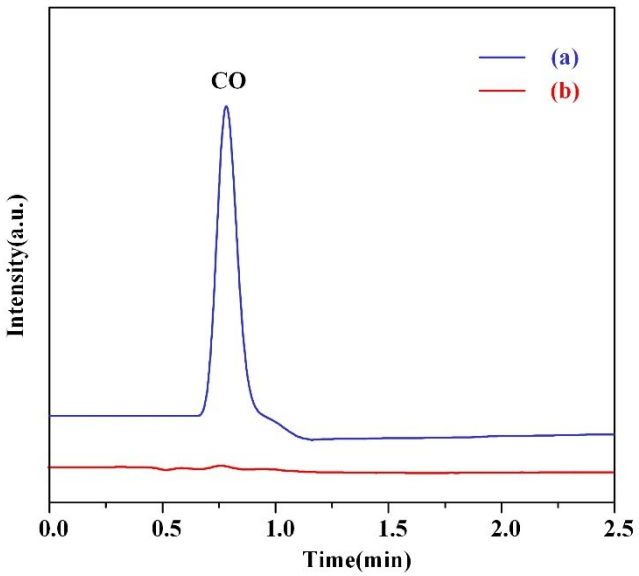

Fig. S3. GC spectrum using FID-Methanator for the a) commercial pure CO, and b) evolved gas from FA/FS aqueous solution (n_{FA} =3 mmol, n_{SF} = 1 mmol) over $Ag_{10}Pd_{90}$/0.2CND/SBA-15 at 323 K.

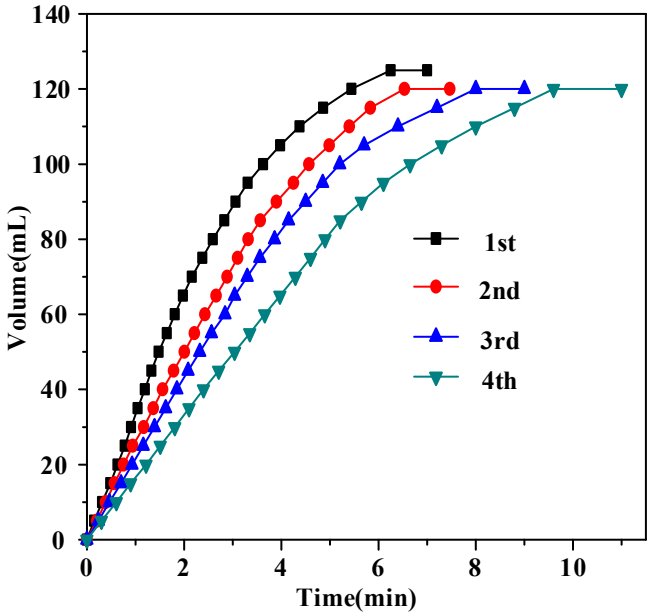

Fig. S4. Stability test on the $Ag_{10}Pd_{90}$/0.2CND/SBA-15 catalyst in the dehydrogenation of FA/SF at 323 K (catalyst= 100 mg, n_{FA} =3 mmol, n_{SF} =1 mmol).

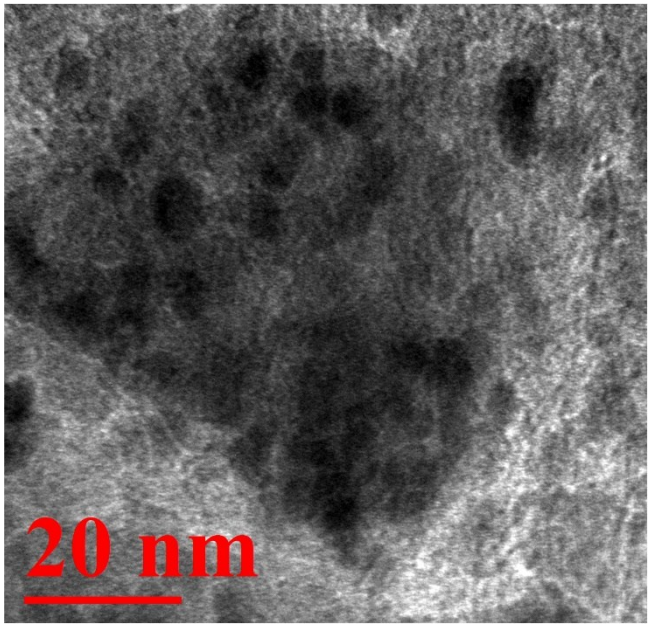

Fig. S5 TEM image of $Ag_{10}Pd_{90}$/0.2CND/SBA-15 after four runs

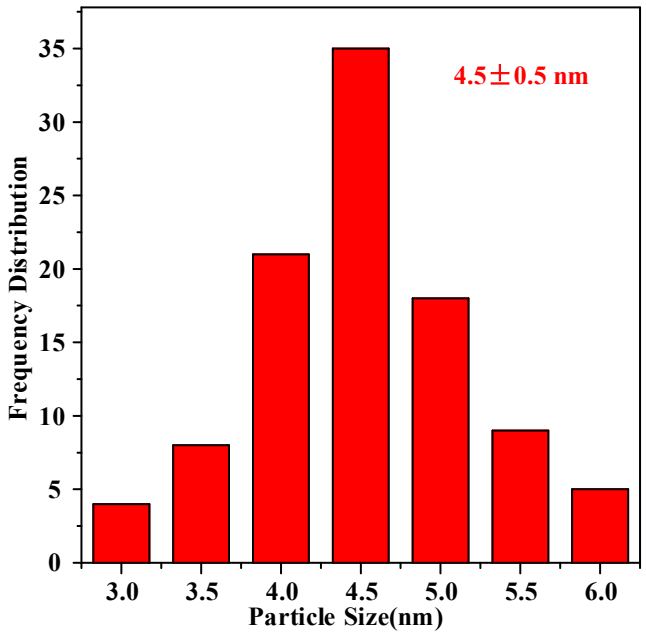

Fig. S6. $Ag_{10}Pd_{90}$ nanoparticle size distribution of $Ag_{10}Pd_{90}$/0.2CND/SBA-15, Mean size = 4.5±0.5 nm.

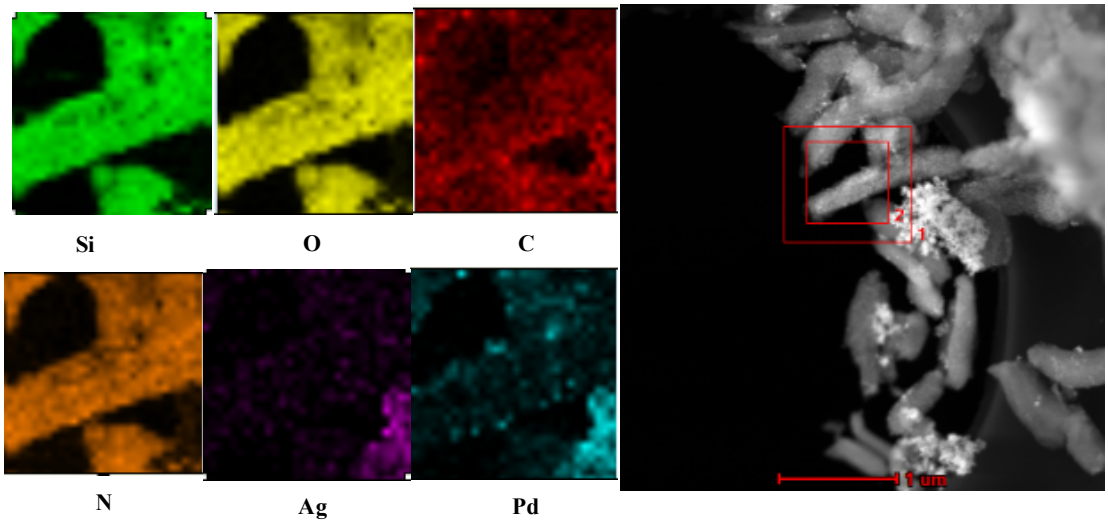

Fig.S7. The corresponding elemental mapping for Si, O, C, N, Ag and Pd elements and HAADF-STEM image of $Ag_{10}Pd_{90}$/0.2CND/SBA-15.

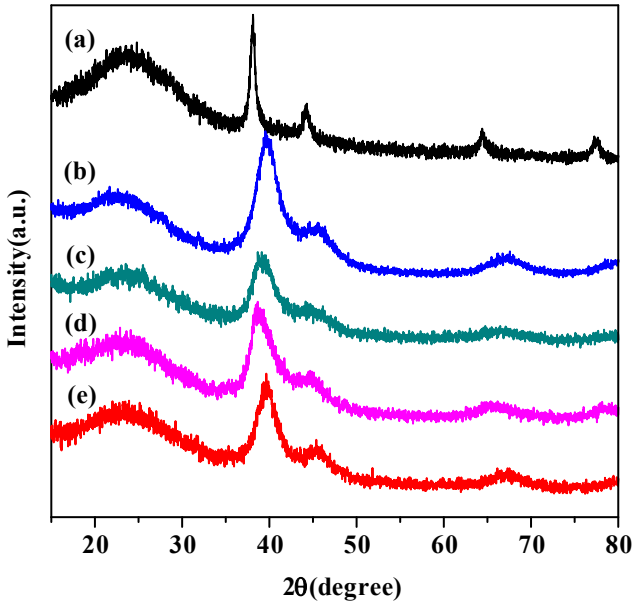

Fig.S8. Wide-angle XRD patterns for (a) Ag/0.2CND/SBA-15, (b) $Ag_{10}Pd_{90}$/0.2CND/SBA-15, (c) $Ag_{20}Pd_{80}$/0.2CND/SBA-15, (d) $Ag_{30}Pd_{70}$/0.2CND/SBA-15 and (e)Pd/0.2CND/SBA-15.

Table S1. ICP-AES results and specific surface area of AgPd/mCND/SBA-15 catalysts

Catalyst	Ag (wt%)	Pd (wt%)	Ag-Pd initial composition	Ag-Pd final composition	Final Metals/Catalyst (mmol/100 mg)	S_{BET}(m^2 g^{-1})
$Ag_{10}Pd_{90}$/0.2CND/SBA-15	0.93	9.26	10:90	9:91	0.096	548
$Ag_{20}Pd_{80}$/0.2CND/SBA-15	1.95	8.16	20:80	19:81	0.095	543
$Ag_{30}Pd_{70}$/0.2CND/SBA-15	3.25	6.78	30:70	32:68	0.094	541
$Ag_{10}Pd_{90}$/SBA-15	1.09	8.68	10:90	11:89	0.092	565
$Ag_{10}Pd_{90}$/0.1CND/SBA-15	0.81	9.17	10:90	8:92	0.094	555
$Ag_{10}Pd_{90}$/0.3CND/SBA-15	1.21	8.68	10:90	12:88	0.093	542
$Ag_{10}Pd_{90}$/0.4CND/SBA-15	1.14	9.06	10:90	11:89	0.096	535

Table. S2 Comparison of AgPd/mCND/SBA-15 catalyzed decomposition of FA/SF solution (n_{FA} =3 mmol, n_{SF} = 1 mmol)

Catalyst	T/ K	Conversion/ %	$TOF_{initial}$/ h^{-1}	H_2/CO_2 ratio
$Ag_{10}Pd_{90}$/0.2CND/SBA-15	323	100	893	1:1
$Ag_{20}Pd_{80}$/0.2CND/SBA-15	323	96.0	609	1:1
$Ag_{30}Pd_{70}$/0.2CND/SBA-15	323	92.0	478	1:1
$Ag_{10}Pd_{90}$/SBA-15	323	92.0	304	1:1
$Ag_{10}Pd_{90}$/0.1CND/SBA-15	323	96.0	638	1:1
$Ag_{10}Pd_{90}$/0.3CND/SBA-15	323	96.0	558	1:1
$Ag_{10}Pd_{90}$/0.4CND/SBA-15	323	92.0	343	1:1

$TOF_{initial}$ is calculated when x_a reaches 20%.